Cancer Letters 305 (2011) 58–68

Contents lists available at ScienceDirect

Cancer Letters

journal homepage: www.elsevier.com/locate/canlet

H_2O_2 scavenging inhibits G1/S transition by increasing nuclear levels of $p27^{KIP1}$

Irene L. Ibañez [a,b,1], Lucía L. Policastro [a,b,1], Ivanna Tropper [c], Candelaria Bracalente [a], Mónica A. Palmieri [d], Paola A. Rojas [b], Beatriz L. Molinari [a,b], Hebe Durán [a,b,c,*]

[a] Comisión Nacional de Energía Atómica, Av. Gral. Paz 1499, (B1650KNA) San Martín, Argentina
[b] Consejo Nacional de Investigaciones Científicas y Técnicas, Argentina
[c] Escuela de Ciencia y Tecnología, Universidad Nacional de San Martín, Argentina
[d] Facultad de Ciencias Exactas y Naturales, Universidad de Buenos Aires, Argentina

ARTICLE INFO

Article history:
Received 4 October 2010
Received in revised form 15 February 2011
Accepted 16 February 2011

Keywords:
Hydrogen peroxide
Cancer cells
Proliferation
Cell cycle
Cyclin D1
$p27^{kip1}$

ABSTRACT

The aim of the present study was to evaluate cell cycle regulation by scavenging H_2O_2 in tumor cells. A significant arrest in the G1 phase of the cell cycle was demonstrated in CH72-T4 carcinoma cells exposed to catalase, associated with a decrease in cyclin D1 and an increase in the CDK inhibitory protein $p27^{KIP1}$. Moreover, we found a differential intracellular distribution of $p27^{KIP1}$, which remained in the nucleus after catalase treatment. *In vivo* experiments showed an increase in nuclear levels of $p27^{KIP1}$ associated with the inhibition of tumor growth by H_2O_2 scavenging, confirming *in vitro* results. To conclude, H_2O_2 scavenging may induce cell cycle arrest through the modulation of cyclin D1 and $p27^{KIP1}$ levels and nuclear localization of $p27^{KIP1}$. To our knowledge, this is the first report that demonstrates that the modulation of ROS alters the intracellular localization of a key regulatory protein of G1/S transition.

1. Introduction

Reactive oxygen species (ROS) can exert different effects according to their nature and to their intracellular levels [1]. Particularly, exposure to moderate levels of H_2O_2 can increase the growth of many types of mammalian cells, whereas scavenging of H_2O_2 inhibits cell proliferation [2–4]. However, high levels of H_2O_2 can induce apoptosis [5], terminal differentiation [6] or cytotoxicity [5].

Increased levels of ROS have been associated with numerous pathological conditions, such as: atherosclerosis and cardiovascular diseases, autoimmune and neurodegenerative disorders and cancer [7]. ROS may play a role in tumor development, both as DNA-damaging agents that increase the mutation rate and promote oncogenic transformation [8] and also as mediators of signal transduction pathways related to cell proliferation [2,4,9], angiogenesis [10] and migration [11]. McCord suggested that a cell

Abbreviations: CDK, cyclin-dependent kinase; CDKI, cyclin-dependent kinase inhibitor; DAPI, 4′,6-diamidine-2′-phenylindole; DCF, dichlorofluorescein; DCFH-DA, 2′,7′-dichlorodihydro-fluorescein diacetate; DMSO, dimethyl sulfoxide; EGFR, epidermal growth factor receptor; ERK1/2, extracellular signal-regulated kinases 1 and 2; FBS, fetal bovine serum; FITC, fluorescein isothiocyanate; MAPKs, mitogen-activated protein kinases; MTT, 3-(4,5-dimethylthiazol-2-y1)-2,5-diphenyltetrazolium bromide; NAC, N-acetyl-L-cysteine; PBS, phosphate buffered saline; PI, propidium iodide; PI3K, phosphatidylinositol 3-kinase; RNase I, ribonuclease I; ROS, reactive oxygen species; RTK, receptor tyrosine kinases; JNK, c-Jun N-terminal kinase; SD, standard deviation; SDS, sodium lauryl sulfate.

* Corresponding author. Address: Comisión Nacional de Energía Atómica, GAIANN, Departamento de Micro y Nanotecnología, Laboratorio de Aplicaciones Biológicas, Av. Gral. Paz 1499, (B1650KNA) San Martín, Provincia de Buenos Aires, Argentina. Tel.: +54 11 6772 7614; fax: +54 11 6772 7134.
E-mail address: hduran@cnea.gov.ar (H. Durán).
[1] These authors contributed equally to this work.

0304-3835/$ - see front matter © 2011 Elsevier Ireland Ltd. All rights reserved.
doi:10.1016/j.canlet.2011.02.026

producing a permanent oxidative shift in the redox status may undergo continuous proliferation that could, in turn, be a crucial event in the appearance of the malignant phenotype [12]. In this sense, the production of large amounts of ROS was reported in tumor cell lines [3,13,14] and in human cancer cells and tissues (breast, colorectal and renal cell carcinoma) as compared with its non-tumoral counterpart [3,14–16]. A correlation between the endogenous levels of H_2O_2 and the degree of malignancy was demonstrated in epithelial tumor cell lines from skin, breast [3] and bladder [17]. In addition, many chemical carcinogens act through free radical metabolites [18], some tumor promoters stimulate the production of free radicals in several cell types and tissues [19], whereas free radical-scavengers protect against cancer development in animal models [20] and may be chemoprotective in humans [18,19].

Regarding the regulation of cell proliferation by ROS, particularly H_2O_2, the inhibition of cell proliferation in tumor cells treated with exogenous catalase or transfected with cDNA of catalase was demonstrated [3,21]. It is well documented that H_2O_2 is involved in signal transduction pathways [22,23], e.g. increased levels of H_2O_2 induce mitogenic signals, such as those related to epidermal growth factor receptor (EGFR)/Ras/ERK1/2 pathway, and stress-responsive signals, such as those related to JNKs and p38 MAPK pathways [22–24].

Cell cycle progression pathways are the endpoint of signaling cascades implicated in cell proliferation. Cell cycle regulation is highly coordinated by sequential assembly and activation of phase-specific protein kinase complexes [25,26], formed by cyclins and cyclin-dependent kinases (CDKs), which are also regulated by the INK4 proteins and the CDK inhibitors (CDKIs). D-type cyclins are expressed throughout the cycle in response to mitogen stimulation [26]. Cyclin D-CDK4 and cyclin E-CDK2 complexes are required for the passage from G1 to S phase. The CDKI $p27^{KIP1}$ is a critical negative regulator of CDK2 and G1/S cell cycle progression [26,27]. The levels of this CDKI are high in quiescent cells, fall in response to mitogenic stimulation, remain at threshold levels in proliferating cells, and increase again when mitogens are withdrawn [26].

It has been reported that fluctuations observed in the intracellular redox state during cell cycle progression could link oxidative metabolic processes to cell cycle regulation [28,29]. H_2O_2 fluctuations along the cell cycle were associated with the regulation of cyclin D1 expression [30]. In contrast, removal of endogenous H_2O_2 by overexpression of catalase and glutathione peroxidase induces G0/G1 arrest [21] and decreases cell DNA synthesis [31]. However, the mechanisms involved in this cell cycle regulation by H_2O_2 have not been fully understood.

In the present study, cell cycle regulatory proteins analysis was performed in response to catalase treatments *in vitro* and *in vivo*. We demonstrated that the scavenging of H_2O_2 by catalase induced G1/S arrest by modulating the levels of specific regulatory proteins of early to mid G1 (cyclin D1) and G1/S transition ($p27^{KIP1}$). Moreover, we found a modification in the intracellular localization of $p27^{KIP1}$. This protein remained in the nucleus after catalase treatment, whereas it showed cytoplasmic localization in proliferating cells. In addition, we demonstrated an increase of $p27^{KIP1}$ in response to H_2O_2 scavenging *in vivo* related to the inhibition of tumor growth after catalase treatment in agreement with *in vitro* results.

2. Materials and methods

2.1. Cell culture and treatments

CH72-T4 cell line was kindly donated by Dr. C. Conti, MD Anderson Cancer Center, University of Texas, USA. CH72-T4 was obtained by four passages *in vivo* of CH72 cells in nude mice and CH72 cell line was originally derived from a squamous cell carcinoma obtained by two stage carcinogenesis in SENCAR mice [32]. Cells were grown in Ham's F12 medium (Invitrogen, # 21700-075) supplemented with 10% fetal bovine serum (FBS) (Natocor), 50 U/ml penicillin and 50 μg/ml streptomycin at 37 °C in a 5% CO_2 humidified atmosphere. Cells were regularly tested to be mycoplasma-free.

For H_2O_2 scavenging experiments, cells were incubated with complete culture medium containing 0–1000 U/ml catalase (Sigma, C9322) for periods of 6 or 24 h. A solution of catalase in phosphate buffered saline (PBS) sterilized by filtration was prepared fresh just before addition to the medium. Considering that H_2O_2 can diffuse across membranes, the addition of catalase to the culture medium will produce a decrease in the intracellular level of H_2O_2 reaching a lower steady state concentration inside and outside the cell [22,30].

2.2. Determination of ROS

The levels of intracellular ROS were determined by 2′,7′-dichlorodihydro-fluorescein diacetate (DCFH-DA, Molecular Probes, D-399) assay. Cells treated with catalase for 24 h or left untreated (control) were washed twice with PBS and incubated with 10 μM DCFH-DA in PBS at 37 °C for 30 min, protected from light. After incubation, cells were washed with PBS, harvested with trypsin/EDTA and evaluated by flow cytometry (FACSCalibur, Becton Dickinson). Ten thousand cells were measured for each experimental condition. To appraise the specificity of H_2O_2 determination by this technique, control cells were treated with 1000 U/ml catalase throughout the assay, added just before DCFH-DA incubation. Data were analyzed with WinMDI software. Three experiments were performed with triplicates per each experimental condition.

For microscopic detection of ROS levels, cells treated with catalase for 24 h, left untreated or FBS starved control cells were incubated with DCFH-DA for 15 min and analyzed under an epifluorescence microscope (Olympus BX51). For each treatment condition, dichlorofluorescein (DCF) and light microscopy images were serially captured by a CCD camera (Olympus DP70) and more than 50 fields were stored containing approximately 20 cells each. An average of 250 cells was randomly screened per experimental condition from the stored images. The mean fluorescence of each cell was quantified by using the NIH Image J software. Three independent experiments were performed with triplicates per condition.

2.3. Cell growth and cell cycle analysis

Cells growing in 24-well plates were treated with catalase or left untreated (control) and the 3-(4,5-dimethylthiazol-2-y1)-2,5-diphenyltetrazolium bromide (MTT, Sigma, M2128) growth assay [33] was performed at 24 h post-treatment as previously described [3]. FBS starved cells were used as control of the inhibition of cell growth. Results were expressed as percentage of inhibition of proliferation, referred to untreated control cells. All experiments were performed at least three times with quadruplicate measurement per condition.

Cell cycle analysis was performed by propidium iodide (PI) staining. Subconfluent cells with or without catalase treatment for 24 h were trypsinized, collected by centrifugation, and washed with ice-cold PBS before fixing in 96% ethanol at 4 °C. Fixed cells were resuspended in 0.2 ml PBS containing 50 μg/ml RNase I (Sigma, R4875) and 60 μg/ml PI (Sigma, P4170). FBS starved cells were used as control of G1 arrest. The number of cells in the different phases of the cell cycle was determined by flow cytometry (FACSCalibur, Becton Dickinson). Ten thousand cells were measured per experimental condition and analyzed with WinMDI and Cylchred software. Three experiments were performed with triplicates per experimental condition.

2.4. Determination of cell cycle regulatory proteins by Western blot

Cells were treated with 500 or 1000 U/ml catalase or left untreated for 6 or 24 h. FBS starved cells were used as control of G1 arrest. To obtain cell extracts, cells were incubated on ice for 30 min in RIPA lysis buffer (Sigma, R0278) containing the Halt protease and phosphatase inhibitor cocktail (Thermo Scientific, #1861281). The protein yield was quantified by the DC Protein Assay Reagent (BioRad, # 500-0114) based on the Lowry protocol. Samples were separated by SDS polyacrylamide (Promega) gel electrophoresis, transferred to nitrocellulose membranes (Hybond ECL Membrane, Amersham Biosciences, GE Healthcare, RPN303D) and immunoblotted by appropriate antibodies.

The antibodies against cyclin D1 (C-20), cyclin E (M-20), CDK4 (C-22), CDK2 (M-2), $p27^{KIP1}$ (M-197) and actin (I-19) were purchased from Santa Cruz Biotechnology. The primary antibodies were detected using horseradish peroxidase-linked donkey anti-rabbit IgG (Amersham, GE Healthcare, NA934V) or anti-goat IgG (Santa Cruz Biotechnology, sc-2020) and visualized by the ECL detection system (Amersham Biosciences, GE Healthcare, RPN2132). Three independent experiments were performed with duplicates per experimental condition.

2.5. Detection of cyclin D1 and $p27^{KIP1}$ by immunofluorescence

Subconfluent cell cultures grown in 60 mm dishes with or without catalase treatment during 6 or 24 h were fixed in 4% (w/v) paraformaldehyde in PBS for 15 min. Cells were then washed with PBS, permeabilized with 0.5% (v/v) Triton X-100 in PBS for 15 min, washed and blocked with 5% (v/v) FBS in PBS for 30 min. Cells were incubated overnight at 4 °C with the polyclonal anti-cyclin D1 (A-12) or anti-$p27^{KIP1}$ (M-197) antibodies (Santa Cruz Biotechnology), 1:300 in PBS, washed and incubated with secondary FITC-conjugated anti-mouse or anti-rabbit IgG (Sigma, F6257 and F9887) for 1 h in the dark at room temperature. Finally, the samples were washed, counterstained and mounted with 1 μg/ml 4′,6-diamidine-2′-phenylindole (DAPI, Sigma, D8417) in an antifade solution in the dark. Cells were examined in an Olympus BX51 epifluorescence microscope utilizing immersion oil with a 100× (UPlanApo 100 X/1.35 oil) objective lens. For each treatment condition, FITC and DAPI images were serially captured by a CCD camera (Olympus DP70) and more than 50 fields containing approximately 20 cells each were stored. A code number was given to each image. Random sampling methods were used to select the images and all the cells in each selected image were screened. An average of 250 cells was evaluated per experimental condition. Total cells, positive cells, positive cytoplasms and positive nuclei for cyclin D1 and $p27^{KIP1}$ were counted by eye by two scorers and results were crosschecked. Three independent experiments were performed with triplicates per condition.

2.6. In vivo experiments

Six-week-old female SENCAR mice and athymic nude (nu^-/nu^-) mice were obtained from the CNEA animal facility (Buenos Aires, Argentina). Animals were kept under conventional housing conditions. Animal care and experimental procedures were conducted in accordance with national and international policies. In order to evaluate the *in vivo* effect of catalase treatment, two experimental tumor models were used: (1) Tumors were induced in athymic nude mice by injecting 1×10^6 CH72-T4 cells subcutaneously (s.c.) in one flank. After 10 days, when tumors were easily detectable (5 ± 2.1 mm^3), animals were treated with catalase during 2 weeks. (2) Tumors were induced in the dorsal skin of SENCAR mice by two stage carcinogenesis, i.e. initiation by a single topical application of 20 nmol of DMBA (Sigma, D3254)/mouse and promotion by multiple applications of 2 μg of TPA (Sigma, P8139)/mouse twice weekly. When tumors appeared, after 2 months of promotion, animals were treated with catalase, in addition to promotion treatment during 5 weeks.

For both experimental tumor models, catalase in PBS was prepared fresh and sterilized by filtration just before treatment. Catalase was injected (1 mg/g body weight) subcutaneously under the tumors three times a week. Since H_2O_2 crosses membranes, catalase in the vicinity of the tumor will favor the decrease of both, extracellular and intracellular levels of H_2O_2. Control animals were treated with PBS or with heat-inactivated catalase in PBS. Three independent experiments were performed with five animals per experimental condition.

2.7. Evaluation of tumor growth and cell proliferation in vivo

Tumor growth was evaluated by measuring tumor volume throughout the complete treatment. Tumor volume for both experimental models was determined by

measurement of the smallest and largest dimensions of tumors with a caliper, twice a week. Volumes were calculated by using the equation: $V = (a \times b^2)/2$, where V is the tumor volume, a is the larger dimension and b is the smaller dimension. Tumor growth was determined for each tumor by calculating the ratio V_x/V_i, where V_x is the volume at day x and V_i is the volume of the same tumor at the first day of treatment.

Two days after the last treatment day, mice were sacrificed and tumors were removed, fixed in 10% neutral buffered formalin, embedded in paraffin, cut at 5 μm and the tissue sections were placed onto silane-coated microscope slides and processed for histopathological examination and immunohistochemistry.

Mitotic index was determined in tissue sections stained with hematoxylin–eosine (H–E) under light microscopy observation by calculating the ratio between the number of cell in mitosis and the total number of cells counted in ten random fields per sample at original magnification 400× with a 10 × 10 squared grid.

2.8. Detection of $p27^{KIP1}$ by immunohistochemistry

Five-micrometer-tissue sections were deparaffinized with xylene, rehydrated through a series of graded alcohols and incubated with 1% (v/v) hydrogen peroxide in methanol for inhibition of endogenous peroxidase. Microwave antigen retrieval was performed by placing the slides in 10 mM citrate buffer (pH 6.0) for 10 min. Tissue sections were blocked with 1% bovine serum albumine in PBS and incubated overnight at 4 °C with a polyclonal anti-$p27^{KIP1}$ antibody (C-19, Santa Cruz Biotechnology), 1:100 in PBS, washed and incubated with the biotin–streptavidine–peroxidase detection system (Super Sensitive Link-Label IHC Detection System RTU Multilink HRP kit, Biogenex, HK340-5K) at room temperature. A solution of 0.7 mg/ml of 3,3′-diaminobenzidine and 0.2 mg/ml of Urea–H_2O_2 in 60 mM Tris buffer (pH 7.6) (SIGMAFAST™ 3,3′-diaminobenzidine tablets, Sigma, D4168) was used as chromogen and peroxidase substrate to detect the staining reaction. For negative controls, the primary antibody was omitted and substituted for PBS. After immunostaining, sections were counterstained with 10% hematoxylin in distilled water, dehydrated and mounted.

The immunohistochemical staining was evaluated by means of light microscopic examination and interpreted by two independent observers who were blinded to the experimental protocol. The final consensus was discussed and determined in a common session. The tumors cells whose nuclei showed antigen expression were interpreted as positive regardless of the staining intensity. Nuclei with positive stained exhibited brown deposits that contrasted with unlabeled blue, hematoxylin-stained, nuclei. Ten random fields were measured at 400× magnification on one section for each tumor. Approximately 250 cells were counted in each evaluated random field.

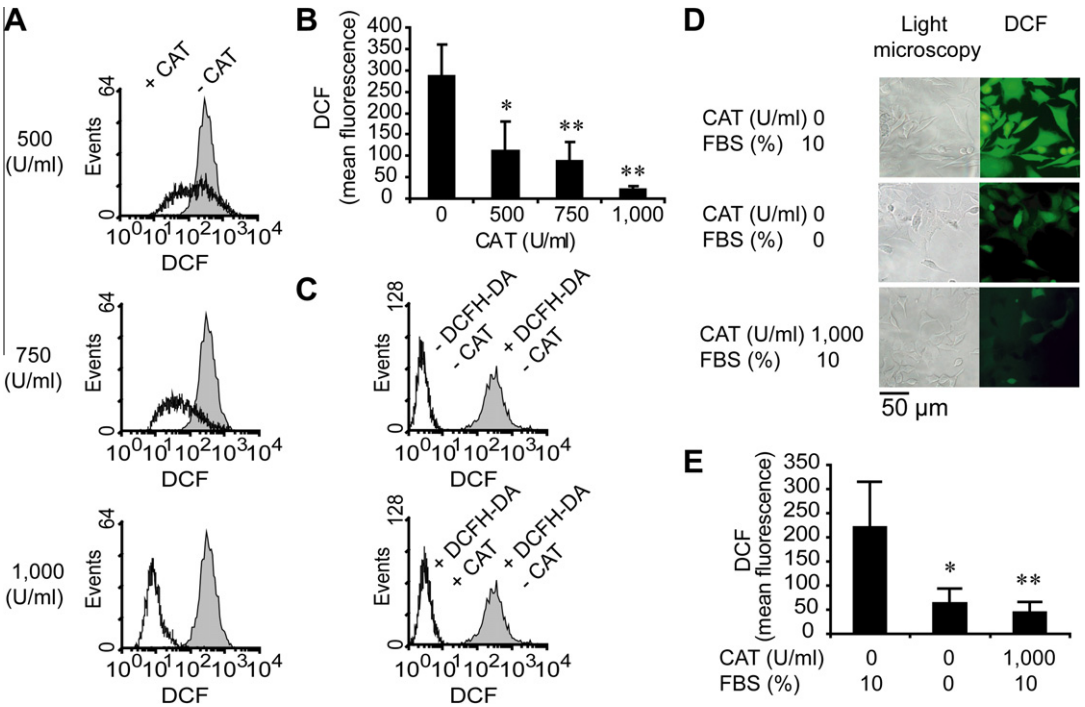

Fig. 1. Decrease of intracellular ROS levels after catalase treatment in CH72-T4 cells determined by DCFH-DA assay. (A) Representative histograms of DCF fluorescence of cells treated with catalase (+CAT) or left untreated (−CAT) for 24 h. (B) DCF mean fluorescence (arbitrary units) vs. catalase (CAT) dose. Data are expressed as mean ± SD. $^{*}p < 0.05$ and $^{**}p < 0.01$ vs. control. (C) The decrease in intracellular ROS levels can be specifically attributed to H_2O_2 scavenging. Control cells were incubated with catalase (+CAT) during the assay. Representative histograms are shown. (D–E) Intracellular ROS levels decreased in FBS starved control cells (FBS 0%) vs. untreated control cells (FBS 10%) (D) Representative images of DCF fluorescence and light microscopy photomicrographs. (E) Quantification of DCF mean fluorescence (arbitrary units), data are expressed as mean ± SD. $^{*}p < 0.05$ and $^{**}p < 0.01$ vs. untreated control.

2.9. Statistical analysis

Data are presented as mean ± SD. Significant changes were assessed using one-way analysis of variance followed by Tukey's multiple comparisons test to determine significant differences between group means. For tumor growth analysis, when parametric tests were not possible to apply, Friedman test for matched observations was performed followed by Dunns multiple comparisons test. *P*-values less than 0.05 were considered significant for all tests.

3. Results

3.1. Inhibition of cell proliferation induced by catalase treatment is mediated by G1 arrest

Intracellular levels of ROS were measured by DCFH-DA assay in CH72-T4 cells treated with catalase and a significant decrease of the mean fluorescence levels of DCF was observed as a function of catalase dose (61%, 70% and 92% for cells treated with 500, 750 and 1000 U/ml, respectively) (Fig. 1A and 1B). Control cells incubated with 1000 U/ml catalase throughout the assay resulted in a 99% decrease of the mean fluorescence levels of DCF (Fig. 1C), showing that the results obtained in response to catalase treatments in our model can be specifically attributed to the scavenging of H_2O_2. The determination of the intracellular levels of ROS in FBS starved cells (Fig. 1D and E) showed significant differences in DCF mean fluorescence ($p < 0.05$) vs. control untreated cells but no significant differences compared to catalase-treated cells.

The decrease in the levels of H_2O_2 induced by catalase treatment resulted in a significant inhibition ($p < 0.01$) of cell proliferation (69%, 85% and 98% for cells treated with 500, 750 and 1000 U/ml, respectively) (Fig. 2A). To further characterize the inhibition of cell proliferation by H_2O_2 scavenging, the distribution of cells in cell cycle phases was analyzed. A significant G1 cell cycle arrest ($p < 0.05$) was induced in CH72-T4 cells by catalase treatment at 24 h (Fig. 2B and 2C).

3.2. G1 cell cycle arrest by H_2O_2 scavenging is mediated by a decrease in cyclin D1 and an increase in $p27^{KIP1}$ levels

In order to evaluate the mechanism by which the scavenging of H_2O_2 induced cell cycle arrest in G1 phase, the levels of the regulatory proteins of G1/S cyclin D1, cyclin E, CDK4, CDK2 and $p27^{KIP1}$ were evaluated by western blot in cells treated with catalase. A significant decrease in cyclin D1 levels (Fig. 3A and 3B) and a significant increase in $p27^{KIP1}$ levels (Fig. 3C and 3D) were observed in CH72-T4 cells treated with catalase in comparison with non-treated cells. The levels of $p27^{KIP1}$ increased 2 and 2.8-fold in cells treated with 1000 U/ml catalase for 6 h and 24 h respectively ($p < 0.01$) (Fig. 3C and 3D).

No significant differences in cyclin E, CDK2 and CDK4 levels ($p > 0.05$) were observed between cells incubated with catalase and non-treated cells (Fig. 3A and 3B).

These results demonstrate that the modulation of two key proteins in the regulation of the G1/S transition, cyclin D1 and $p27^{KIP1}$, was involved in the inhibition of cell proliferation by catalase treatment.

3.3. $p27^{KIP1}$ is localized in the nucleus after catalase treatment

Regarding the subcellular localization of cyclin D1, the percentage of positive CH72-T4 cells for this protein was evaluated by immunofluorescence in response to H_2O_2 scavenging during 6 or 24 h (Fig. 4). The signal for cyclin D1 was extremely low in the nucleus of cells treated with catalase and a significant decrease of the percentage of positive nuclei was found in these cells as compared with control untreated cells ($p < 0.01$). These results agree with the western blot ones. Therefore, the H_2O_2 scavenging would block the cell cycle at early G1 by avoiding the expression of cyclin D1.

Considering that the subcellular localization of the inhibitory protein $p27^{KIP1}$ is a critical event in its regulatory activity, the effect of H_2O_2 scavenging on the localization of this protein was studied by immunofluorescence in CH72-T4 cells treated with catalase during 6 or 24 h. Consistent with the western blot results, positive cells for $p27^{KIP1}$ expression

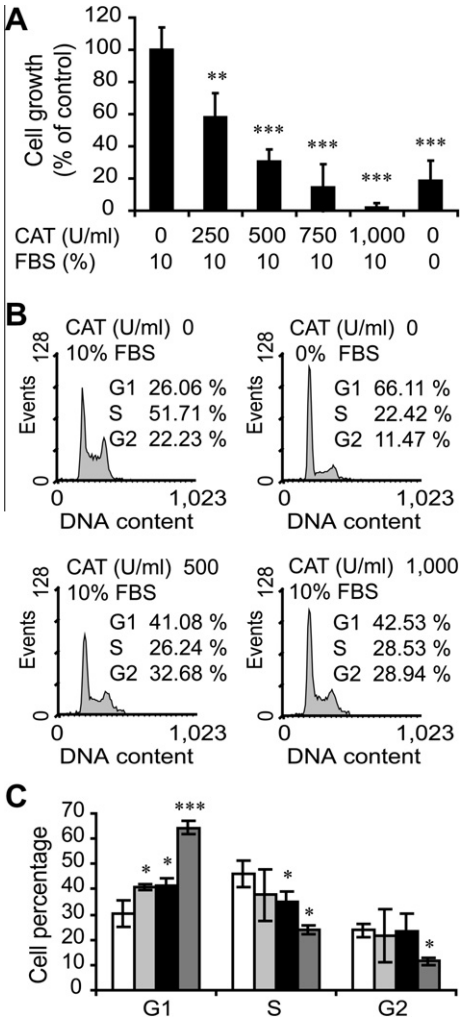

Fig. 2. Inhibition of CH72-T4 cell proliferation and cell cycle arrest induced by catalase treatment. (A) Percentage of cell proliferation after catalase (CAT) treatment for 24 h, relative to control cells, evaluated by the MTT assay. Data are expressed as mean ± SD. (B and C) Cell cycle analysis assessed by flow cytometry after staining with propidium iodide. (B) Representative histograms of DNA content of cells treated with: 0–1000 U/ml CAT during 24 h. (C) Percentage of cells in the different phases of the cell cycle in response to CAT treatment. FBS starved cells were used as control of G1 arrest. (□) Untreated control cells, (▒) 500 U/ml and (■) 1000 U/ml CAT and (▓) FBS starved cells. Data are expressed as mean ± SD. $^{*}p < 0.05$, $^{**}p < 0.01$ and $^{***}p < 0.001$ vs. untreated control.

increased in catalase-treated cells as compared with the untreated cells ($p < 0.05$ for 500 U/ml and $p < 0.01$ for 1000 U/ml of catalase-treated cells). Remarkably, this protein was localized primarily within the nucleus in cells incubated with catalase ($p < 0.001$) in comparison with untreated cells, in which $p27^{KIP1}$ distribution was predominantly cytoplasmic (Fig. 5). Thus, the persistence of $p27^{KIP1}$ in the nucleus induced by catalase treatment would favor the inhibition of the cyclin E-CDK2 complex, blocking the G1/S transition.

3.4. In vivo inhibition of tumor growth is induced by catalase treatment

In order to study the effect of *in vivo* treatment with catalase on tumor growth, tumors were induced by injecting CH72-T4 cells in nude mice or by a two stage carcinogenesis protocol as described in Section

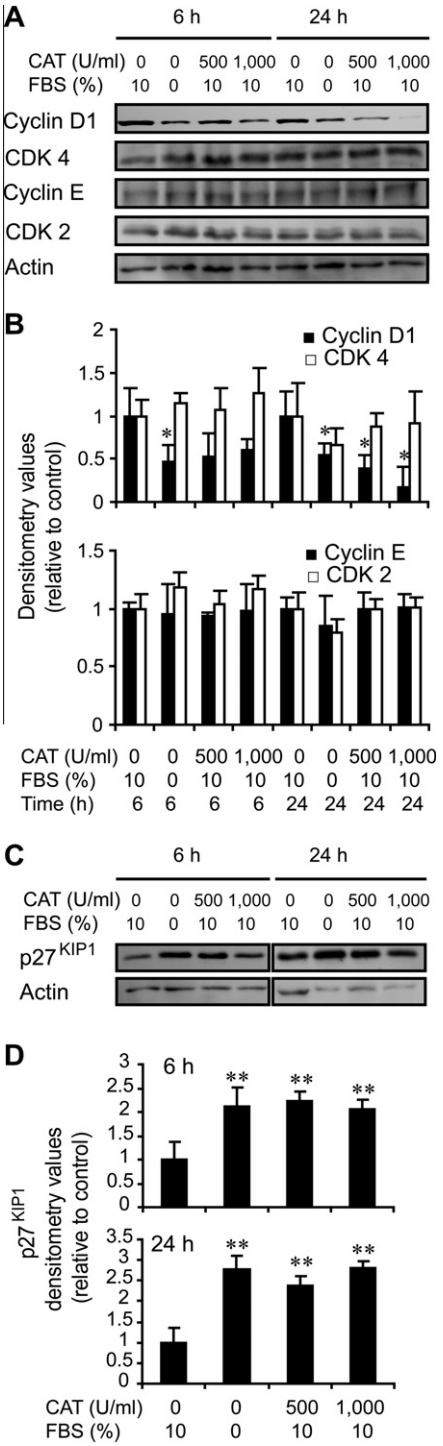

Fig. 3. Decrease of cyclin D1 and increase of $p27^{KIP1}$ levels in response to H_2O_2 scavenging. The expression of G1/S regulatory proteins in CH72-T4 cells treated with catalase (CAT) for 6 and 24 h was analyzed by western blot. FBS starved cells were used as control of G1 arrest. (A and C) Representative immunoblot images. Actin densitometric values were used to standardize for protein loading. (B) Relative densitometric values of cyclins and CDKs levels. (D) Relative densitometric values of $p27^{KIP1}$ levels. (B and D) Quantification was performed by densitometric scanning with the NIH Image J software. Results are referred to control without treatment. Data are expressed as mean ± SD. $^{*}p < 0.05$ and $^{**}p < 0.01$ vs. untreated control.

2. Treatments with catalase resulted in a significant inhibition of tumor growth in both experimental models (Fig. 6A), consistent with our *in vitro* results. The evaluation of tumor volumes throughout the treatments demonstrated a significant decrease in tumor growth in catalase treated mice ($p < 0.01$) as compared with both control conditions (heat-inactivated catalase or PBS treated mice). Moreover, no new tumors were detected in mice treated with the two stage carcinogenesis protocol from the onset of the catalase treatment (Fig. 6B). There were no significant differences between non-treated and inactivated catalase-treated animals in both experimental models.

Representative images of tissue sections of tumor specimens stained with H–E are shown in Fig. 7A and B. The tumors of mice treated with catalase in both experimental models exhibited a significant decrease in the mitotic index as compared with both control tumors ($p < 0.01$) revealing the inhibition of cell proliferation in response to H_2O_2 scavenging (Fig. 7C and 7D). No significant differences in the mitotic index were obtained between non-treated and heat-inactivated catalase treated tumors in both experimental models.

3.5. H_2O_2 scavenging induced an increase of nuclear $p27^{KIP1}$ levels in vivo

Considering the results of *in vitro* experiments for $p27^{KIP1}$, we analyzed the detection of this inhibitory protein by immunohistochemistry in tissue sections of tumor specimens of mice treated with catalase, heat-inactivated catalase or PBS. A significant increase in the percentage of positive nuclei for $p27^{KIP1}$ was observed in tumors of animals treated with catalase ($p < 0.001$) as compared with both control conditions in both experimental models (Fig. 8). Moreover, control tumors exhibited low signal of $p27^{KIP1}$ with predominant cytoplasmic localization. These results confirmed our *in vitro* findings.

4. Discussion

In this study we demonstrated an increase in the levels of the CDK inhibitory protein $p27^{KIP1}$ and a modification in its intracellular localization induced by H_2O_2 scavenging in a model of squamous cell carcinoma *in vitro* and *in vivo*. Moreover, a decrease in cyclin D1 protein levels was found after catalase treatment. The modulation of these two key regulatory proteins of G1/S transition, cyclin D1 and $p27^{KIP1}$, resulted in G1 arrest and the inhibition of proliferation and tumor growth.

Remarkably, high levels of $p27^{KIP1}$ were found in the nucleus after catalase treatment as compared with proliferating control cells. Considering that $p27^{KIP1}$ is a negative regulator of the CDK2–cyclin E complex [26,27], the persistence of this regulatory protein in the nucleus would be a critical event in blocking the G1/S transition by scavenging H_2O_2.

Laurent et al. [4] reported that the growth of normal cells is triggered by oxidant signals directed to growth-related genes, up to a critical threshold beyond which ROS become cytotoxic. Moreover, the constitutive levels of endogenous ROS in tumor cells are close to that threshold. These authors showed that the increased generation of ROS in tumor cell lines resulted from both an elevated mitochondrial production and a marked decrease in the activity of antioxidant enzymes. In agreement with these results, in a previous report [3], we demonstrated higher levels of H_2O_2 production in the carcinoma cell line CH72-T4 as compared with a near normal cell line (PB cells) of the same origin, concomitant with an imbalance in the antioxidant system, an increase in the levels of SOD and a decrease of H_2O_2-detoxifying enzymes, catalase and glutathione peroxidase. We showed herein that catalase treatment in CH72-T4 cells induced an arrest in the G1

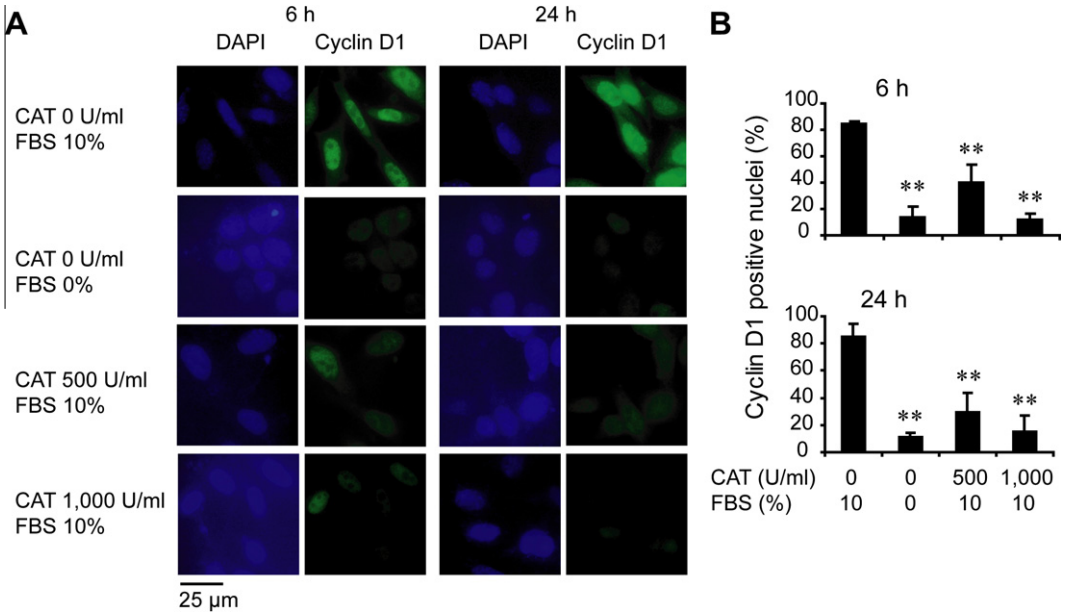

Fig. 4. Nuclear decrease of cyclin D1 in CH72-T4 cells treated with catalase. Cyclin D1 was detected by immunocytofluorescence in cells treated with 500 and 1000 U/ml catalase (CAT) for 6 or 24 h or left untreated. FBS starved cells were used as control of G1 arrest. (A) Representative images of cyclin D1 immunocytofluorescence. DAPI: staining of nuclear DNA. Cyclin D1: FITC staining of cyclin D1 protein. (B) Percentage of positive cells for cyclin D1 relative to the total number of counted cells. Data are expressed as mean ± SD. $^{**}p < 0.01$ vs. untreated control.

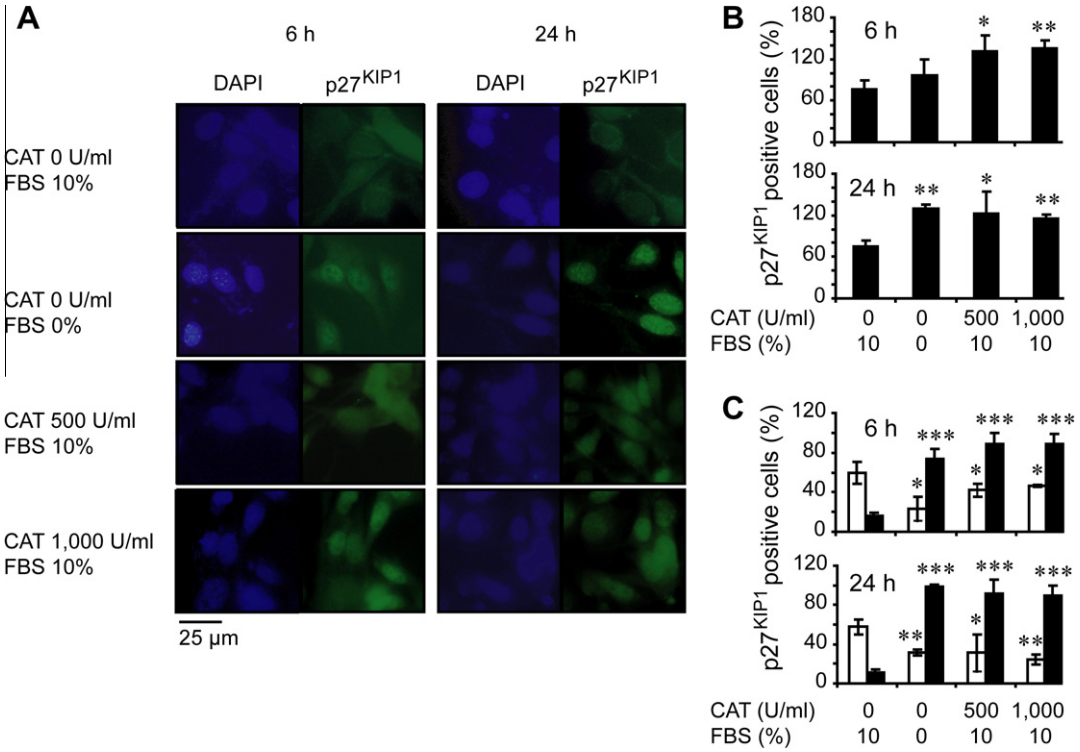

Fig. 5. Nuclear localization of $p27^{KIP1}$ in CH72-T4 cells after H_2O_2 scavenging. $p27^{KIP1}$ was detected by immunocytofluorescence in cells treated with 500 and 1000 U/ml catalase (CAT) for periods of 6 or 24 h or left untreated. FBS starved cells were used as control of G1 arrest. (A) Representative images of $p27^{KIP1}$ immunocytofluorescence showing the subcellular localization of the protein. DAPI: staining of nuclear DNA; $p27^{KIP1}$: FITC staining of $p27^{KIP1}$ protein. (B) Percentage of positive cells for $p27^{KIP1}$ relative to the total number of counted cells. (C) Percentage of positive (■) nuclei and positive (□) cytoplasms for $p27^{KIP1}$relative to the total number of counted cells. (B and C) Data are expressed as mean ± SD. $^{*}p < 0.05$, $^{**}p < 0.01$ and $^{***}p < 0.001$ vs. untreated control.

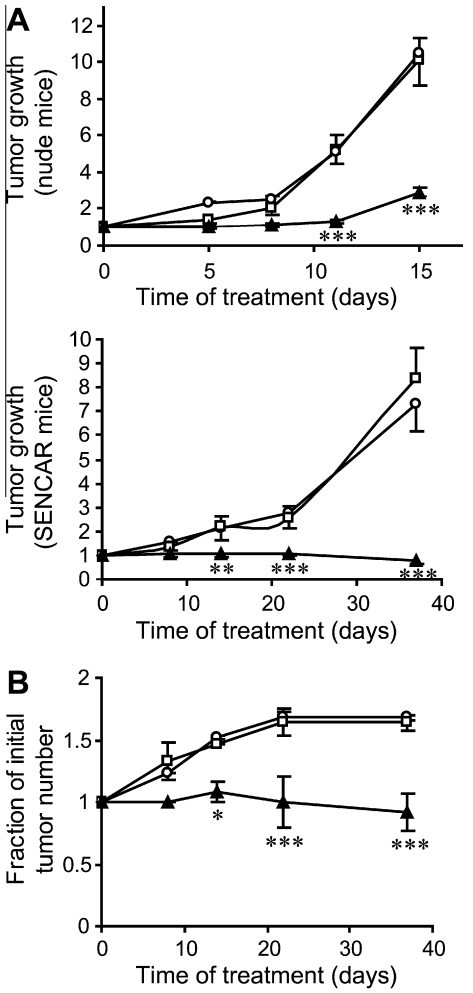

Fig. 6. *In vivo* inhibition of tumor growth by treatment with catalase (1 mg/g) in nude mice inoculated with CH72-T4 cells and in SENCAR mice exposed to a two stage carcinogenesis protocol. (A) Tumor volume was normalized to 1 at the onset of treatment with catalase. Individual tumor growth was monitored throughout treatment. (B) Variation in the total number of tumors in SENCAR mice during catalase treatment expressed as the increasing fraction of the initial number of tumors. (○) PBS control, (□) heat-inactivated catalase and (▲) catalase. Data are expressed as mean ± SD. $^{*}p < 0.05$, $^{**}p < 0.01$ and $^{***}p < 0.001$ vs. PBS control.

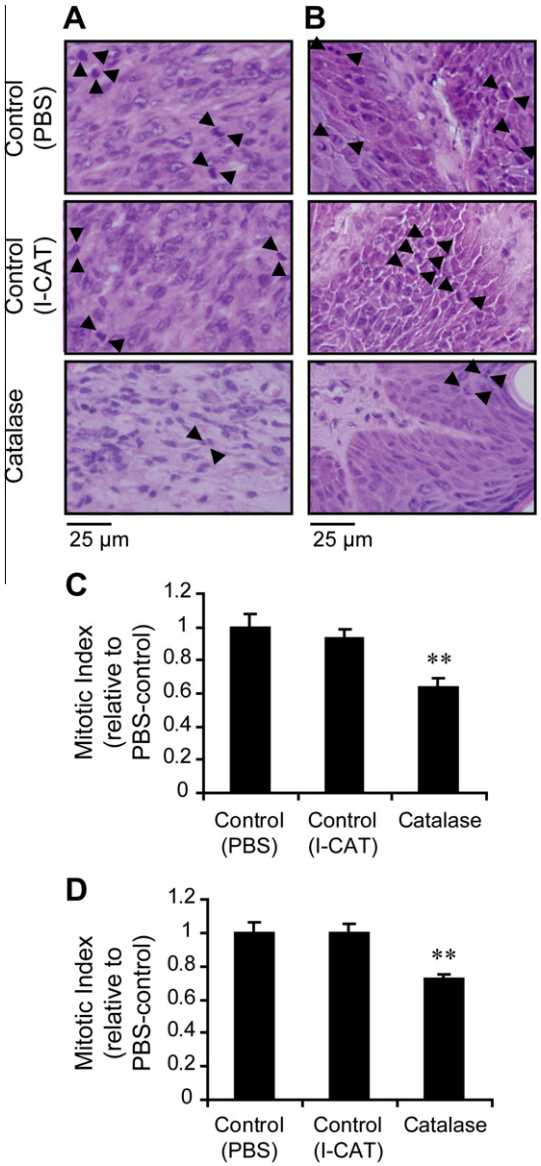

Fig. 7. Mitotic index decrease in tumors of mice treated with catalase. (A and C) Nude mice. (B and D) SENCAR mice. (A and B) Representative images of tumor tissue specimens stained with H–E. Arrows indicate cells in mitosis. (C and D) Mitotic index evaluated in tissue sections stained with H–E of tumor specimens treated with catalase, heat-inactivated catalase (I-CAT) or PBS. Data are expressed as mean ± SD. $^{**}p < 0.01$ vs. PBS control.

phase of the cell cycle. Our results accord with other reports that show the association between G1 arrest and decreased ROS levels in other experimental conditions [21,28,31,34,35]. This blockage of the cell cycle shown *in vitro* is consistent with the inhibition of tumor growth and the decrease in the mitotic index demonstrated *in vivo*.

ROS generated by cellular metabolism and by receptor activation induced by growth factors act as secondary messengers in numerous signaling pathways governing cellular processes, including proliferation. In this sense, growth factors trigger H_2O_2 production that leads to mitogen-activated protein kinases (MAPKs) activation [23]. This could explain the decrease in ROS levels observed in FBS starved cells in our model. It has been previously demonstrated that the pathways that promote mitogenesis through ROS converge at the level of transcription of the cyclin D1 gene, which has been considered as a functional marker of G0 to G1 transition [30]. Once cells are actively cycling, ROS may encourage proliferation by maintaining cyclin D1 levels [30], a key regulatory protein in the growth factor-induced G1 progression. It was also found that upon scavenging of extracellular H_2O_2, ERK1/2 activity was lowered and JNK1 activity was increased [36]. Moreover, there is evidence of the requirement of sustained ERK activity in the regulation of the continued expression of cyclin D1 [37]. In our experimental model, we found a

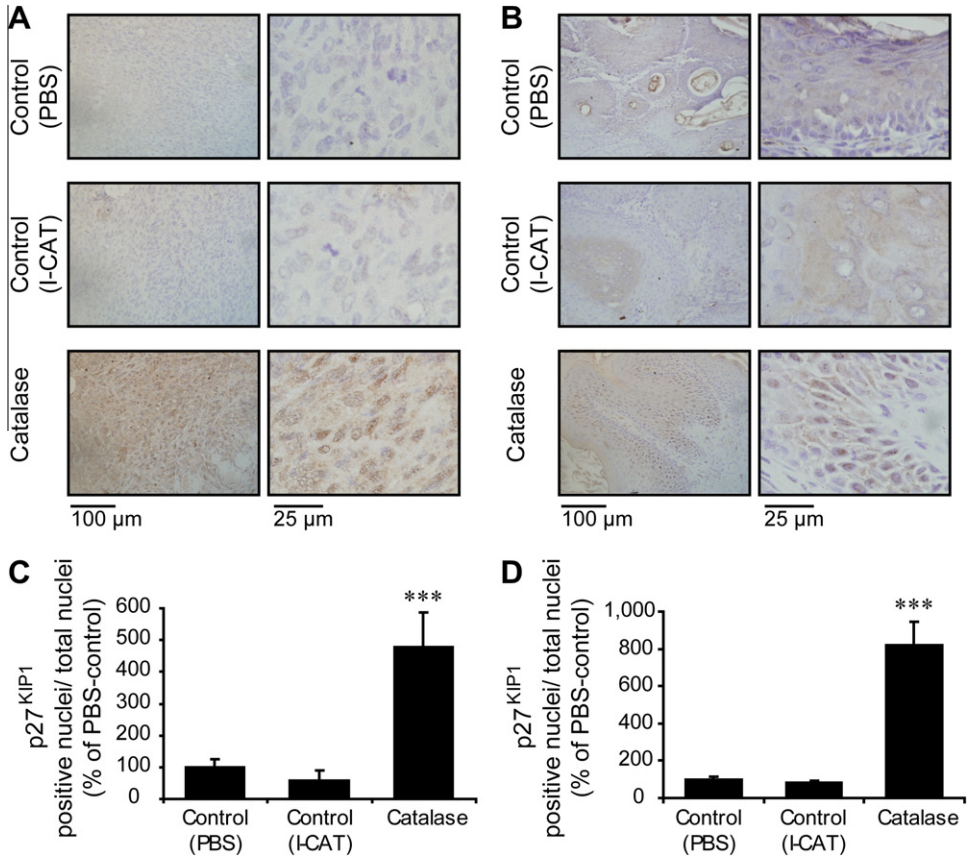

Fig. 8. Increase of nuclear levels of $p27^{KIP1}$ after catalase treatment *in vivo*. Detection of $p27^{KIP1}$ by immunohistochemistry in tissue sections of tumor specimens of nude (A and C) or SENCAR (B and D) mice treated with catalase, heat-inactivated catalase (I-CAT) or PBS. (A and B) Representative images of $p27^{KIP1}$ immunohistochemistry. (C and D) Percentage of $p27^{KIP1}$ positive nuclei per total number of counted nuclei relative to PBS control. Data are expressed as mean ± SD. $^{***}p < 0.001$ vs. PBS control.

decrease in the levels of cyclin D1 associated with the inhibition of proliferation induced by the scavenging of H_2O_2. We suggest that this modulation of cyclin D1 would be the result of the inhibition of the ERK1/2 activity, induced by lowering the levels of extracellular H_2O_2. Our results are in agreement with Menon et al. [38], who showed G1 arrest with decreased cyclin D1 protein levels in mouse fibroblasts treated with the thiol antioxidant *N*-acetyl-L-cysteine (NAC). On the other hand, sublethal doses of exogenous H_2O_2 (250 μM) induce cell cycle arrest in fibroblasts by the down-regulation of cyclin D1 and D3 [39]. Thus, the growth inhibitory effect of both high levels of H_2O_2 and H_2O_2 scavenging treatments would be mediated by a decrease in cyclin D1.

Overexpression of cyclin D1 has been reported in different types of human and experimental tumors [40,41]. Several lines of evidence indicate that cyclin D1 is involved in the proliferative response to oncogenic Ras [42]. Moreover, the expression of cyclin D1 may be stimulated by activated ras through MAPKs pathways [43]. In particular, the overexpression of cyclin D1 has been described in mouse skin tumors induced by a two stage carcinogenesis protocol [41], which have a characteristic oncogenic mutation in codon 61 of the Ha-ras gene [42]. Thus, the decrease in cyclin D1 that we observed in CH72-T4 cells treated with catalase could be explained by the inhibition of H_2O_2-mediated signals involved in the Ras/MAPKs cascade.

Regarding the CDKs inhibitory protein $p27^{KIP1}$, it plays a critical role in cell cycle regulation by virtue of its ability to respond to changes in the growth environment of the cell, integrating diverse signals into a final decision between proliferation and cell cycle exit [26,27].

The activities of $p27^{KIP1}$ are controlled by its concentration, subcellular localization and phosphorylation status [26]. This protein remains in the nucleus in quiescent cells, but it is exported to the cytoplasm for its degradation in response to proliferating signals [27]. In the present study, we demonstrated the increase of this regulatory protein after catalase treatment and a differential intracellular localization as compared to proliferating cells. The scavenging of H_2O_2 induced the nuclear localization of $p27^{KIP1}$, whilst control proliferating cells showed mainly cytoplasmic localization of this protein. To our knowledge, this is the first report that shows the modulation of the intracellular localization of $p27^{KIP1}$ mediated by ROS levels *in vitro* and *in vivo*.

It has been previously described that Ras activity is required for the suppression of $p27^{KIP1}$ levels in proliferat-

ing cells [44]. Then, the high proliferation activity found in CH72-T4 cells could be explained by the characteristic activating mutation of the Ha-ras gene described in this carcinogenesis model [42] that would be involved in lowering levels of $p27^{KIP1}$ through signaling pathways downstream of Ras. Particularly, the activation of MAPKs pathways is required for $p27^{KIP1}$ down-regulation and for G0/G1 transition [44,45]. Moreover, it has been well established that the control of $p27^{KIP1}$ levels is mostly due to the rate of degradation [27]. MAPK (ERK1/2) activation accelerates $p27^{KIP1}$ proteolysis by inducing the translocation of this protein from the nucleus to the cytoplasm, followed by its degradation [27,46]. Thus, the higher levels and the nuclear localization of $p27^{KIP1}$ that we found after catalase treatment could be the result of the inhibition of ERK1/2 induced by H_2O_2 scavenging [36].

However, both the regulation of the activities and the mechanism of $p27^{KIP1}$ removal are extremely complex. This protein may be phosphorylated at multiple sites and contains at least 6–8 phosphorylatable residues; several kinases have been reported as being responsible for these phosphorylations [27]. Most of these post-translational modifications are on threonine and serine residues [46]. However, phosphorylations on tyrosine residues have recently been reported [47,48]. A number of reports converge on PI3K/AKT as a pivotal pathway in the regulation of $p27^{KIP1}$ levels, localization and regulatory activities of cyclin–CDKs complexes [46,49–51]. Regarding the modification on tyrosine residues, phosphorylations within the CDK-binding domain of $p27^{KIP1}$ by oncogenic tyrosine kinases were reported [46,47,51], which impairs the CDK2 inhibitory action of $p27^{KIP1}$. It has been shown that the inhibition of protein tyrosine phosphatases by ROS may directly trigger tyrosine kinases activity [7]. Thus, considering that ROS have been described as mediators of RTK/Ras, MAPKs, PI3K/AKT and non-receptor tyrosine kinases pathways [7], the scavenging of H_2O_2 would be preventing $p27^{KIP1}$ degradation or nuclear $p27^{KIP1}$ export. In view of this complex regulation, further studies are needed to determine the status of phosphorylatable residues of $p27^{KIP1}$ after catalase treatment, to elucidate the mechanisms by which this protein increased its concentration and remained in the nucleus in response to H_2O_2 scavenging.

Considering that cyclin D1 may regulate the cyclin E/CDK2 complex through its capacity to sequester CDK inhibitors such as $p27^{KIP1}$ and by preventing the inhibition of this complex by $p27^{KIP1}$ [26,27], we conclude that both the decrease in cyclin D1 levels and the increase in the levels and the nuclear localization of $p27^{KIP1}$ that we found after catalase treatment would favor the blockage of the G1/S transition by the inhibition of the cyclin E/CDK2 complex.

Although $p27^{KIP1}$ is rarely mutated or deleted in cancer, it is frequently deregulated: $p27^{KIP1}$ protein levels are reduced or the protein is mislocalized [46]. We suggest that this deregulation observed in most cancers be explained by the permanent shift in the redox status, characteristic of cancer cells [13–17], which would in turn be responsible for activating ROS-dependent signaling cascades involved in the regulation of phosphorylation and degradation of $p27^{KIP1}$.

6. Conflict of interest

None declared.

Acknowledgments

This work was supported in part by grants from ANPCyT, Argentina (PICT 2007-01628 and PICT 05-14330) and Fundación Florencio Fiorini. CB and IT are doctoral fellows of ANPCyT and ANPCyT–UNSAM respectively. The authors thank Víctor H. Tomasi for the technical advice provided in immunohistochemistry and María E. Ibalo for her valuable assistance. Moreover, the authors gratefully acknowledge Dr. María L. Paparella for her contribution to histopathological examination and wish to express our thanks to Andrea C. Cruz for proofreading our work and advising us on the use of English language.

References

[1] K.J. Davies, Oxidative stress, antioxidant defenses, and damage removal, repair, and replacement systems, IUBMB Life 50 (2000) 279–289.
[2] R.S. Arnold, J. Shi, E. Murad, A.M. Whalen, C.Q. Sun, R. Polavarapu, S. Parthasarathy, J.A. Petros, J.D. Lambeth, Hydrogen peroxide mediates the cell growth and transformation caused by the mitogenic oxidase Nox1, Proc. Natl. Acad. Sci. USA 98 (2001) 5550–5555.
[3] L. Policastro, B. Molinari, F. Larcher, P. Blanco, O.L. Podhajcer, C.S. Costa, P. Rojas, H. Durán, Imbalance of antioxidant enzymes in tumor cells and inhibition of proliferation and malignant features by scavenging hydrogen peroxide, Mol. Carcinog. 39 (2004) 103–113.
[4] A. Laurent, C. Nicco, C. Chéreau, C. Goulvestre, J. Alexandre, A. Alves, E. Lévy, F. Goldwasser, Y. Panis, O. Soubrane, B. Weill, F. Batteux, Controlling tumor growth by modulating endogenous production of reactive oxygen species, Cancer Res. 65 (2005) 948–956.
[5] F. Antunes, E. Cadenas, Cellular titration of apoptosis with steady state concentrations of H_2O_2: submicromolar levels of H_2O_2 induce apoptosis through Fenton chemistry independent of the cellular thiol state, Free Radical Biol. Med. 30 (2001) 1008–1018.
[6] M.C. Carreras, D.P. Converso, A.S. Lorenti, M. Barbich, D.M. Levisman, A. Jaitovich, V.G. Antico Arciuch, S. Galli, J.J. Poderoso, Mitochondrial nitric oxide synthase drives redox signals for proliferation and quiescence in rat liver development, Hepatology 40 (2004) 157–166.
[7] M. Valko, D. Leibfritz, J. Moncol, M.T. Cronin, M. Mazur, J. Telser, Free radicals and antioxidants in normal physiological functions and human disease, Int. J. Biochem. Cell Biol. 39 (2007) 44–84.
[8] B. Halliwel, Oxidative stress and cancer: have we moved forward?, Biochem J. 401 (2007) 1–11.
[9] K. Irani, Y. Xia, J.L. Zweier, S.J. Sollot, C.J. Der, E.R. Fearon, M. Sundaresan, T. Finkel, P.J. Goldschmidt-Clermont, Mitogenic signaling mediated by oxidants in ras-transformed fibroblasts, Science 275 (1997) 1649–1652.
[10] M. Ushio-Fukai, Redox signaling in angiogenesis: role of NADPH oxidase, Cardiovasc. Res. 71 (2006) 226–235.
[11] K.K. Nelson, A.C. Ranganathan, J. Mansouri, A.M. Rodriguez, K.M. Providence, J.L. Rutter, K. Pumiglia, J.A. Bennett, J.A. Melendez, Elevated sod2 activity augments matrix metalloproteinase expression: evidence for the involvement of endogenous hydrogen peroxide in regulating metastasis, Clin. Cancer Res. 9 (2003) 424–432.
[12] J.M. McCord, Superoxide radical: controversies, contradictions, and paradoxes, Proc. Soc. Exp. Biol. Med. 209 (1995) 112–117.
[13] T.P. Szatrowski, C.F. Nathan, Production of large amounts of hydrogen peroxide by human tumor cells, Cancer Res. 51 (1991) 794–798.
[14] L.L. Policastro, I.L. Ibañez, H.A. Durán, G. Soria, V. Gottifredi, O.L. Podhajcer, Suppression of cancer growth by nonviral gene therapy based on a novel reactive oxygen species-responsive promoter, Mol. Ther. 17 (2009) 1355–1364.
[15] S. Toyokuni, K. Okamoto, J. Yodoi, H. Hiai, Persistent oxidative stress in cancer, FEBS Lett. 358 (1995) 1–3.

[16] S. Kondo, S. Toyokuni, Y. Iwasa, T. Tanaka, H. Onodera, H. Hiai, M. Imamura, Persistent oxidative stress in human colorectal carcinoma, but not in adenoma, Free Radical Biol. Med. 27 (1999) 401–410.
[17] N. Hempel, H. Ye, B. Abessi, B. Mian, J.A. Melendez, Altered redox status accompanies progression to metastatic human bladder cancer, Free Radical Biol. Med. 46 (2009) 42–50.
[18] K.Z. Guyton, T.W. Kensler, Oxidative mechanisms in carcinogenesis, Br. Med. Bull. 49 (1993) 523–544.
[19] P.A. Cerutti, Prooxidant states and tumor promotion, Science 227 (1985) 375–381.
[20] K. Hyoudou, M. Nishikawa, M. Ikemura, Y. Kobayashi, A. Mendelsohn, N. Miyazaki, Y. Tabata, F. Yamashita, M. Hashida, Prevention of pulmonary metastasis from subcutaneous tumors by binary system-based sustained delivery of catalase, J. Controlled Release 137 (2009) 110–115.
[21] O.E. Onumah, G.E. Jules, Y. Zhao, L. Zhou, H. Yang, Z. Guo, Overexpression of catalase delays G0/G1- to S-phase transition during cell cycle progression in mouse aortic endothelial cells, Free Radical Biol. Med. 46 (2009) 1658–1667.
[22] J.R. Stone, S. Yang, Hydrogen peroxide: a signaling messenger, Antioxid. Redox Signal. 8 (2006) 243–270.
[23] Y. Cakir, S.W. Ballinger, Reactive species-mediated regulation of cell signaling and the cell cycle: the role of MAPK, Antioxid. Redox Signal. 7 (2005) 726–740.
[24] M. Benhar, D. Engelberg, A. Levitzki, ROS, stress-activated kinases and stress signaling in cancer, EMBO Rep. 3 (2002) 420–425.
[25] S.J. Elledge, Cell cycle checkpoints: preventing an identity crisis, Science 274 (1996) 1664–1672.
[26] C.J. Sherr, Cancer cell cycles, Science 274 (1996) 1672–1677.
[27] A. Borriello, V. Cucciola, A. Oliva, V. Zappia, F. Della Ragione, $p27^{KIP1}$ metabolism: a fascinating labyrinth, Cell Cycle 6 (2007) 1053–1061.
[28] S.G. Menon, E.H. Sarsour, D.R. Spitz, R. Higashikubo, M. Sturm, H. Zhang, P.C. Goswami, Redox regulation of the G1 to S phase transition in the mouse embryo fibroblast cell cycle, Cancer Res. 63 (2003) 2109–2117.
[29] E.H. Sarsour, M.G. Kumar, L. Chaudhuri, A.L. Kalenand, P.C. Goswami, Redox control of the cell cycle in health and disease, Antioxid. Redox Signal. 11 (2009) 2985–3011.
[30] P.M. Burch, N.H. Heintz, Redox regulation of cell-cycle re-entry: cyclin D1 as a primary target for the mitogenic effects of reactive oxygen and nitrogen species, Antioxid. Redox Signal. 7 (2005) 741–751.
[31] Q. Felty, K.P. Singh, D. Roy, Estrogen-induced G1/S transition of G0-arrested estrogen-dependent breast cancer cells is regulated by mitochondrial oxidant signaling, Oncogene 24 (2005) 4883–4893.
[32] C.J. Conti, J.W. Fries, A. Viaje, D.R. Miller, R. Morris, T.J. Slaga, In vivo behavior of murine epidermal cell lines derived from initiated and noninitiated skin, Cancer Res. 48 (1988) 435–439.
[33] Y. Liu, D.A. Peterson, H. Kimura, D. Schubert, Mechanism of cellular 3-(4,5-dimethylthiazol-2-y1)-2,5-diphenyltetrazolium bromide (MTT) reduction, J. Neurochem. 69 (1997) 581–593.
[34] X. Deng, F. Gao, W.S. May JrJr., Bcl2 retards G1/S cell cycle transition by regulating intracellular ROS, Blood 102 (2003) 3179–3185.
[35] V. Martín, F. Herrera, G. García-Santos, I. Antolín, J. Rodriguez-Blanco, C. Rodriguez, Signaling pathways involved in antioxidant control of glioma cell proliferation, Free Radical Biol. Med. 42 (2007) 1715–1722.
[36] T.J. Preston, W.J. Muller, G. Singh, Scavenging of extracellular H_2O_2 by catalase inhibits the proliferation of HER-2/Neu-transformed rat-1 fibroblasts through the induction of a stress response, J. Biol. Chem. 276 (2001) 9558–9564.
[37] J.D. Weber, D.M. Raben, P.J. Phillips, J.J. Baldassare, Sustained activation of extracellular-signal-regulated kinase 1 (ERK1) is required for the continued expression of cyclin D1 in G1 phase, Biochem. J. 326 (1997) 61–68.
[38] S.G. Menon, E.H. Sarsour, A.L. Kalen, S. Venkataraman, M.J. Hitchler, F.E. Domann, L.W. Oberley, P.C. Goswami, Superoxide signaling mediates N-acetyl-L-cysteine-induced G1 arrest: regulatory role of cyclin D1 and manganese superoxide dismutase, Cancer Res. 67 (2007) 6392–6399.
[39] K. Barnouin, M.L. Dubuisson, E.S. Child, S. Fernandez de Mattos, J. Glassford, R.H. Medema, D.J. Mann, E.W. Lam, H_2O_2 induces a transient multi-phase cell cycle arrest in mouse fibroblasts through modulating cyclin D and p21Cip1 expression, J. Biol. Chem. 277 (2002) 13761–13770.
[40] E. Tashiro, A. Tsuchiya, M. Imoto, Functions of cyclin D1 as an oncogene and regulation of cyclin D1 expression, Cancer Sci. 98 (2007) 629–635.
[41] A.I. Robles, C.J. Conti, Early overexpression of cyclin D1 protein in mouse skin carcinogenesis, Carcinogenesis 16 (1995) 781–786.
[42] M.L. Rodríguez-Puebla, A.I. Robles, C.J. Conti, Ras activity and cyclin D1 expression: an essential mechanism of mouse skin tumor development, Mol. Carcinog. 24 (1999) 1–6.
[43] C. Albanese, J. Johnson, G. Watanabe, N. Eklund, D. Vu, A. Arnold, R.G. Pestell, Transforming p21ras mutants and c-Ets-2 activate the cyclin D1 promoter through distinguishable regions, J. Biol. Chem. 270 (1995) 23589–23597.
[44] G. Sa, D.W. Stacey, Stacey P27 expression is regulated by separate signaling pathways, downstream of Ras, in each cell cycle phase, Exp. Cell. Res. 300 (2004) 427–439.
[45] N. Rivard, M.J. Boucher, C. Asselin, G. L'Allemain, MAP kinase cascade is required for p27 downregulation and S phase entry in fibroblasts and epithelial cells, Am. J. Physiol. 277 (1999) C652–C664.
[46] M.D. Larrea, S.A. Wander, J.M. Slingerland, P27 as Jekyll and Hyde: regulation of cell cycle and cell motility, Cell Cycle 8 (2009) 3455–3461.
[47] M. Grimmler, Y. Wang, T. Mund, Z. Cilensek, E.M. Keidel, M.B. Waddell, H. Jäkel, M. Kullmann, R.W. Kriwackiand, L. Hengst, Cdk-inhibitory activity and stability of $p27^{KIP1}$ are directly regulated by oncogenic tyrosine kinases, Cell 128 (2007) 269–280.
[48] I. Chu, J. Sun, A. Arnaout, H. Kahn, W. Hanna, S. Narod, P. Sun, C.K. Tan, L. Hengstand, J. Slingerland, P27 phosphorylation by src regulates inhibition of cyclin E-Cdk2, Cell 128 (2007) 281–294.
[49] G. Viglietto, M.L. Motti, P. Bruni, R.M. Melillo, A. D'Alessio, D. Califano, F. Vinci, G. Chiappetta, P. Tsichlis, A. Bellacosa, A. Fusco, M. Santoro, Cytoplasmic relocalization and inhibition of the cyclin-dependent kinase inhibitor $p27^{KIP1}$ by PKB/Akt-mediated phosphorylation in breast cancer, Nat. Med. 8 (2002) 1136–1144.
[50] J. Liang, J. Zubovitz, T. Petrocelli, R. Kotchetkov, M.K. Connor, K. Han, J.H. Lee, S. Ciarallo, C. Catzavelos, R. Beniston, E. Franssenand, J.M. Slingerland, PKB/Akt phosphorylates p27, impairs nuclear import of p27 and opposes p27-mediated G1 arrest, Nat. Med. 8 (2002) 1153–1160.
[51] M.K. James, A. Ray, D. Leznova, S.W. Blain, Differential modification of $p27^{KIP1}$ controls its cyclin D-cdk4 inhibitory activity, Mol. Cell. Biol. 28 (2008) 498–510.